LBNL-47073
TA-444

ASHRAE Transactions, Vol. 107 (2) 2001

Natural Convection Effects in Three-Dimensional Window Frames with Internal Cavities

Arild Gustavsen, Brent T. Griffith and Dariush Arasteh

Windows and Daylighting Group
Building Technologies Department
Environmental Energy Technologies Division
Ernest Orlando Lawrence Berkeley National Laboratory
University of California
1 Cyclotron Road
Berkeley, CA 94720

October 2000

This work was supported by Hydro Aluminum and the Assistant Secretary for Energy Efficiency and Renewable Energy, Office of Building Technology, State and Community Programs, Office of Building Research and Standards of the U.S. Department of Energy under Contract No. DE-AC03-76SF00098.

DISCLAIMER

CI-01-5-1

Natural Convection Effects in Three-Dimensional Window Frames with Internal Cavities

Arild Gustavsen

Brent T. Griffith
Student Member ASHRAE

Dariush Arasteh, P. E.
Member ASHRAE

ABSTRACT

This paper studies three-dimensional natural convection effects in window frames with internal cavities. Infrared (IR) thermography experiments, computational fluid dynamics (CFD) simulations, and calculations with traditional software for simulating two-dimensional heat conduction were conducted. The IR thermography experiments mapped surface temperatures during steady-state thermal tests between ambient thermal chambers set at 0ºC and 20ºC. Using a non-contact infrared scanning radiometer and an external referencing technique, we were able to obtain surface temperature maps with a resolution of 0.1ºC and 3 mm and an estimated uncertainty of ±0.5ºC and ±3 mm. The conjugate CFD simulations modeled the enclosed air cavities, frame section walls, and foam board surround panel. With the two-dimensional heat conduction simulation software, we used correlations to model heat transfer in the air cavities. For both the CFD simulations and the conduction simulation software, boundary conditions at the external air/solid interface were modeled using constant surface heat-transfer coefficients with fixed ambient air temperatures.

Different cases were studied, including simple, four-sided frame sections (with one open internal cavity), simple vertical sections with a single internal cavity, and horizontal sections with a single internal cavity. The sections tested in the Infrared Thermography Laboratory (IR lab) were made of PVC. Both PVC and thermally broken aluminum sections were modeled. Based on the current investigations, it appears that the thermal transmittance or U-factor of a four-sided section can be found by calculating the average of the thermal transmittance of the respective single horizontal and vertical sections. In addition, we conclude that two-dimensional heat transfer simulation software agrees well with CFD simulations if the natural convection correlations used for the internal cavities are correct.

INTRODUCTION

Natural convection in glazing cavities has been an international research topic for many years. Convective heat-transfer correlations have been determined both from experiments (Shewen et al. 1996; ElSherbiny et al. 1982) and numerical simulations (Zhao 1998; Lee and Korpela 1983). In simulations, a two-dimensional situation usually is assumed and can be justified because of the extensive width of the glazing cavities. The convective heat-transfer correlations that have emerged from experiments also only consider two-dimensional cavities. In contrast, heat transfer in window frames with internal cavities has not received much attention. Only few researchers (Haustermans 2000; Griffith et al. 1998) have reported effects resulting from the natural convection in such frames. Griffith et al. (1998) studied the significance of bolts on the thermal performance of curtain-wall frames but did not focus on the natural convection effects in the internal cavities in detail. Haustermans (2000) measured the thermal performance of two types of thermally broken aluminum window frames with internal cavities in a guarded hot box. Complete (four-sided) window frames, single vertical and single horizontal sections, were tested. Haustermans (2000) found that, for purposes of U-factor calculation, a four-sided frame could be regarded as an assembly of independent vertical and horizontal frame sections. By comparing U-factors, he found that CFD simulations of single horizontal and vertical sections agreed well with experimental results. Simulations with traditional two-dimensional heat-conduction

Arild Gustavsen is a university lecturer in the Department of Building and Construction Engineering, Norwegian University of Science and Technology, Trondheim, Norway. **Brent T. Griffith** is a graduate student research assistant, Massachusetts Institute of Technology, Cambridge, Mass. **Dariush Arasteh** is a staff scientist, Lawerence Berkeley National Laboratory, Berkeley, Calif.

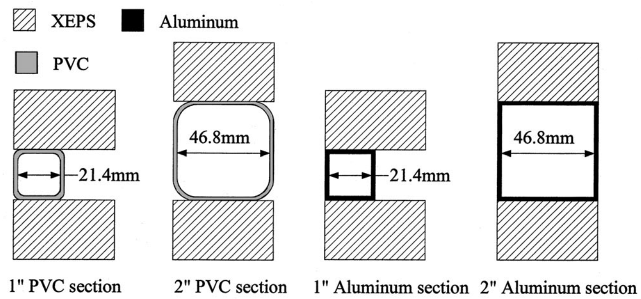

Figure 1 *Cross section of the measured PVC profiles and the modeled thermally broken aluminum profiles mounted in two-inch-thick (50.8 mm) extruded polystyrene panel (XEPS).*

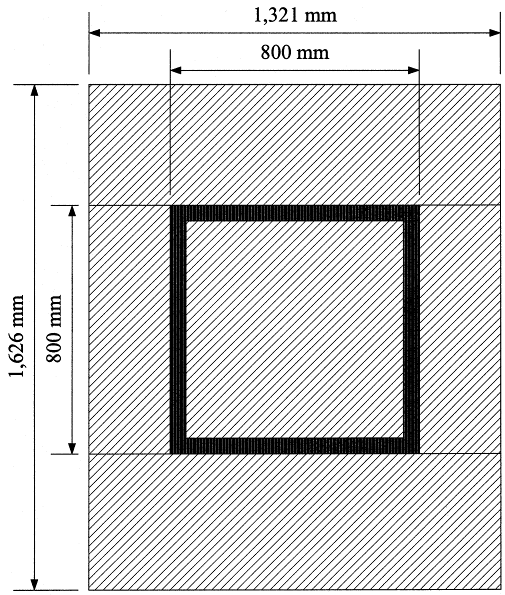

Figure 2 *Mounting of four-sided frame specimen in the XEPS surround panel.The figure is drawn for the dimensions of the two-inch (50.8 mm) frame specimen.*

simulation software also gave U-factors that agreed well with his experimental results if the correct air cavity natural convection correlations were used. However, Haustermans did not study specimen surface temperatures in detail. Surface-temperature studies are important for insight about window frame corner effects and about how natural convection effects in internal cavities develop.

Some researchers will probably claim that each horizontal and vertical portion of a window frame can be approximated in two dimensions. Horizontal sections, because of their width, could be modeled in two dimensions with some accuracy, but for vertical sections, which have narrow cavities, three-dimensional effects are expected. Furthermore, information about entire window frames with internal cavities is lacking and merits research.

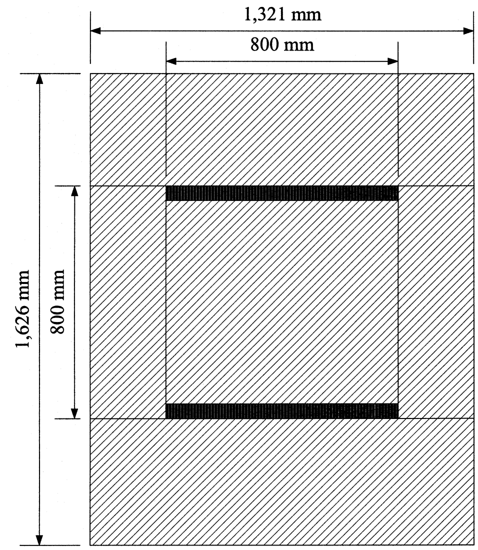

Figure 3 *Mounting of the two horizontal specimens in the XEPS surround panel; the figure is drawn for the dimensions of the two-inch (50.8 mm) PVC profiles.*

This paper looks at different effects that result from natural convection in the internal cavities of thermally broken aluminum window frames and PVC window frames. This is a companion paper to Gustavsen et al. (2001), which discusses validation of window frame cavity CFD simulations by infrared (IR) thermography experiments. As in the investigations for the other report, the work done for this paper is based on IR thermographic experiments and numerical simulations with a computational fluid dynamics (CFD) program. In addition, we performed numerical simulations with a more traditional two-dimensional conductive heat transfer program (Finlayson et al. 1998). Different simple frame configurations were studied.

METHODOLOGY

Window Frame Geometries

Although each specimen studied can be thought of either as a complete window frame or as a component of a complete window frame, the sections we used were not actual window frames but rather standard and custom vinyl (polyvinyl chloride, PVC) extrusions and thermally broken aluminum sections. The cross sections of the specimens are shown in Figure 1. The sections were mounted in extruded polystyrene (XEPS). Complete (four-sided) window frame sections and horizontal and vertical sections were studied. When we refer to four-sided sections, we mean a configuration like the one shown in Figure 2. These sections have open internal cavities so that air can flow freely from the vertical sections to the horizontal sections and vice versa. The horizontal sections were mounted, as shown in Figure 3, to get similar natural convection effects on the warm side as for the four-sided sections. Because the focus of this work is on the window frame rather

TABLE 1
Specimen Descriptions

Description	1-Inch Square Frame	Vertical, 1-inch Section	Horizontal 1-Inch Section	2-Inch Square Frame	Vertical, 2-Inch Section	Horizontal, 2-Inch Section
	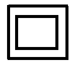	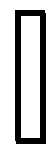		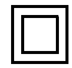	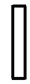	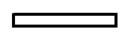
Orientation during test	entire frame	vertical	horizontal	entire frame	vertical	horizontal
Overall height (mm)	800	800	25.4	800	800	800
Overall width (mm)	800	25.4	800	800	50.8	50.8
Outer size of cross section (mm)	25.4	25.4	25.4	50.8	50.8	50.8
Outer depth of frame section (mm)	25.4	25.4	25.4	50.8	50.8	50.8
Wall thickness (mm)	2.0	2.0	2.0	2.0	2.0	2.0
Size of inner cavity (maximum length in heat flow direction) (mm)	21.4	21.4	21.4	46.8	46.8	46.8
H/L aspect ratio	37.2/1	37.4	1	17.0/1	17.1	1
W/L aspect ratio	1/37.2	1	37.4	1/17.0	1	17.1
Maximum Rayleigh number, Ra_{max}	2.4×10^4	2.4×10^4	2.4×10^4	2.5×10^5	2.5×10^5	2.5×10^5

H/L and W/L are based on the inner height H, inner length L, and inner width W. The maximum Rayleigh number, Ra_{max}, is calculated from ΔT = 20ºC, inner length L of the cavity in the heat-flow direction, and air properties at mean temperature T_m = 10ºC.

than on a complete window with glazing, we used XEPS to fill the window frame sections. Different profile sizes were chosen to represent the range of sizes usually found in window frames with internal cavities. Window frames found in actual buildings have several internal cavities; however, we chose the described configuration so that we could determine which cavity caused convection effects when we analyzed the warm-surface temperature data from the experiments. Another reason for choosing simple sections was that we wanted to limit the complexity of the CFD model.

In the experiments, PVC was used for the cavities to allow larger temperature gradients to develop on the surface than would result with a more highly conductive material such as aluminum. Because of the use of PVC and the manufacturing process followed, the edges of the profiles were rounded, as shown for the two sections to the left in Figure 1. In the simulations, however, we modeled the PVC sections with orthogonal corners. Other characteristics of the physical experiments that not were directly modeled include the use of silicone to seal and flatten the warm-side surface of the sections, the presence of paint on the warm-side surface, and the use of vinyl tape on the cold side to form an air seal between the specimen and the surround panel. Thermally broken aluminum frames were also modeled (these were not tested in the IR lab). The aluminum frames had the same dimensions as the PVC sections. The only difference is that the warm and the cold sides of the specimen were aluminum instead of PVC, as shown for the two sections to the right in Figure 1. The conductivity of the thermal break was set to be the same as the conductivity of PVC. The reader is referred to Gustavsen et al. (2001) for a more thorough description of specimen preparation and mounting and a discussion of the differences between the tested specimens and the modeled specimens. The different specimens used in this paper are listed in Table 1 along with their sizes, aspect ratios, and other important properties.

Experiments

The experimental part of this work was conducted at the Infrared Thermography Laboratory (IR lab), which consists of an IR box in which a steady-state heat flow in created through specimens mounted between a climate chamber and a thermography chamber. The climate chamber is used to simulate outside conditions with a given temperature and air velocity across the face of the specimen. The thermography chamber is used to maintain stable conditions on the warm side of the test specimen. The IR box differs from a traditional hot box because there is no baffle in front of the specimen in the ther-

TABLE 2
Material Properties Used in the Computer Simulations

Material	Emissivity	Thermal Conductivity, W/mK
Aluminum	0.9	160
PVC	0.9	0.17
Painted XPS	0.9	0.03

mography chamber. The baffle is omitted to allow for an unobstructed view of the test specimen. An infrared imager with a detector sensitive to thermal radiation in the wavelength interval 8 to 12 µm is used to capture temperature data. A detailed discussion of IR thermography and the external referencing technique used are presented elsewhere (Griffith et al. 1995, 1999; Türler et al. 1997) and thus will not be described in detail here. Below, we give only a short summary of the boundary conditions.

In our experiment we used ISO (1998) conditions; that is, the warm-side bulk air temperature was controlled to 20ºC, and the cold-side bulk air temperature was controlled to 0ºC. Separate experiments, using a calibrated transfer standard (CTS), characterized the performance of the IR box for rates of surface heat transfer. The overall surface heat-transfer coefficient for the cold side was measured at 26 ±5 W/m^{2}K. The overall surface heat-transfer coefficient for the warm side was measured at 7.9 ±0.4 W/m^{2}K.

Computer Simulations

We used a computational fluid dynamics program (Fluent 1998) and a two-dimensional conductive heat-transfer program THERM (Finlayson et al. 1998) for the numerical simulations described in this paper. The CFD program uses a control-volume-based technique to convert the governing equations to algebraic equations that can be solved numerically. The method will not be described in detail; only salient features pertinent to this investigation will be presented. Readers interested in the numerical method are referred to Fluent (1998) and textbooks, i.e., Patankar (1980) or Versteeg and Malalasekera (1995), that describe this technique. THERM 2.0 uses a finite-element approach to solve the governing equations in two dimensions. Correlations are used to model convective heat transfer in air cavities, and view factors or fixed radiation coefficients can be used to calculate radiant heat transfer.

In the CFD program, our conjugate heat transfer problem involves solution of three-dimensional energy, momentum, and continuity equations on a hexahedral mesh. Air flow is assumed to be incompressible. Viscous dissipation is not addressed, and all thermophysical properties are assumed to be constant except for the buoyancy term of the y-momentum equation where the Boussinesq approximation is assumed. In Table 1, we see that the maximum Rayleigh number, Ra_{max}, for the vertical one-inch section is close to the laminar/turbulence limit. Flow changes from laminar to turbulent near Ra = 2×10^4 for two-dimensional cavities where H/L = 40 (Yin et al. 1978). However, the temperature difference between the internal walls of the cavity is likely to be smaller than 20°C, which is the temperature difference used for calculating the maximum Rayleigh number, so the real Rayleigh number is lower. In addition, the turbulence limit is probably higher than Ra = 2×10^4 for a three-dimensional vertical square cavity than for a two-dimensional cavity because of the added restriction imposed on the flow by the narrowness of the cavity. Because we also know that laminar flow simulations performed using the CFD program compared well with IR thermography (Gustavsen et al. 2001), we assumed laminar flow for the simulations in this paper. Radiant heat transfer was included in the simulations by use of the discrete transfer radiation model (DTRM), which relies on a ray-tracing technique to calculate surface-to-surface radiation. The internal cavity walls are assumed to be diffuse gray, and the fluid (air) does not interact with the radiative process. The semi-implicit method for pressure-linked equations consistent (SIMPLEC) was used to model the interaction between pressure and velocity. The energy and momentum variables at cell faces were found the by using the quadratic upstream interpolation for convective kinetics (QUICK) scheme. In addition, the CFD program uses central differences to approximate the diffusion terms and relies on the pressure interpolation scheme pressure staggering option (PRESTO) to find the pressure values at the cell faces. PRESTO is similar to the staggered grid approach described by Patankar (1980). Convergence is determined by checking the scaled residuals and ensuring that they are less than 10^{-5} for all variables except for the energy equation in which the residuals have to be less than 10^{-6}.

TABLE 3
Boundary Conditions Used in the Computer Simulations

	Temperature, ºC	Total Surface Film Coef., W/m^{2}K
Warm side	20	7.69
Cold side	0	25

The material properties and the boundary conditions used in the simulations are given in Tables 2 and 3, respectively. As we see in Table 2, the emissivity of aluminum was set to 0.9, like the emissivity of PVC, so that both sections would have the same radiation properties; this value is close to what we find for anodized aluminum.

RESULTS

Several properties and effects were studied, including warm-side surface temperatures, corner effects, complex flow patterns, and heat-transfer rates. The figures of surface

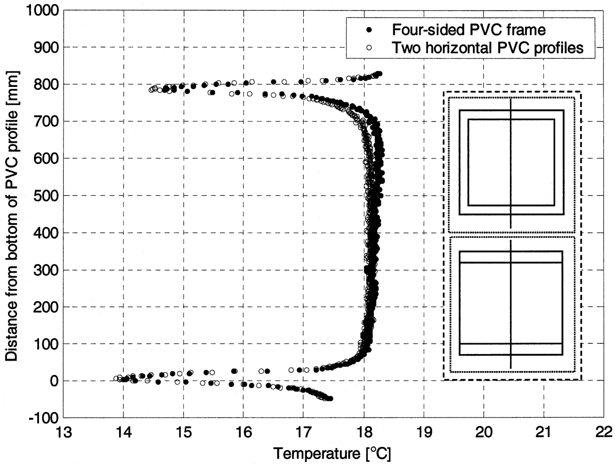

Figure 4 *Surface temperatures down the middle of one-inch-square frame compared to the temperatures down the middle of the two one-inch horizontal PVC profiles; experimental uncertainty is estimated to be ±0.5°C (Griffith and Arasteh 1999).*

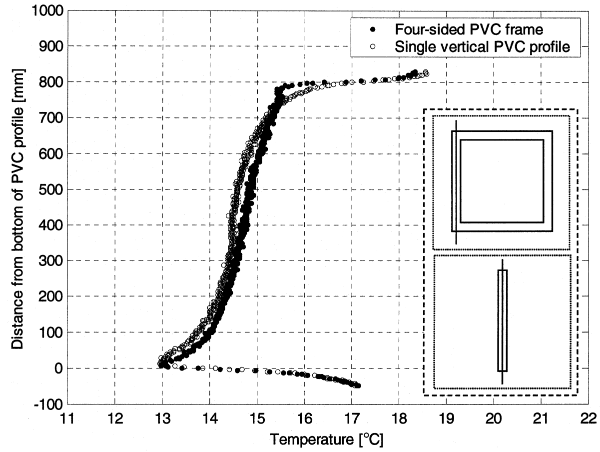

Figure 5 *Temperature along the vertical part of the four-sided one-inch PVC frame compared to the surface temperatures of a single vertical one-inch PVC profile; experimental uncertainty is estimated to be ±0.5°C (Griffith and Arasteh 1999).*

temperature also show schematically the locations on the frame sections where the temperature data were collected. For the heat transfer calculations, three-dimensional CFD simulations and traditional conductive heat-transfer simulations were compared.

Surface Temperature Plots

Figure 4 shows the warm-side surface temperatures along a line down the middle of the one-inch square frame and the pair of one-inch horizontal profiles, which are one-inch versions of the specimens shown in Figures 2 and 3, respectively. Both data sets are from IR thermography experiments. The vertical axis shows the accumulated distance from the lower edge of the bottom profile in millimeters. The lower profile extends from 0 mm to 25.4 mm and the upper profile from 774.6 mm to 800 mm. Outside these areas, data are plotted for the temperature of the foam surround panel in which the specimens were mounted. The horizontal axis shows the surface temperature in °C. The IR data were averaged on each vertical level to reduce noise.

In Figure 5 we see the temperature down the middle of the vertical part of the one-inch square frame compared to the temperature down the middle of a single one-inch vertical profile. The horizontal axis shows the surface temperature in °C, and the vertical axis shows the accumulated distance from the bottom edge of the frame section and the single PVC profile. The bottom edge of the profiles is 0 mm; 800 mm is on the top. Data were averaged on each vertical level to reduce noise; however, because the temperature varies in the horizontal direction, the number of data points averaged was kept to a minimum.

Figure 6 shows a line plot of the temperature along the middle of the lower-left horizontal part (the corner region)

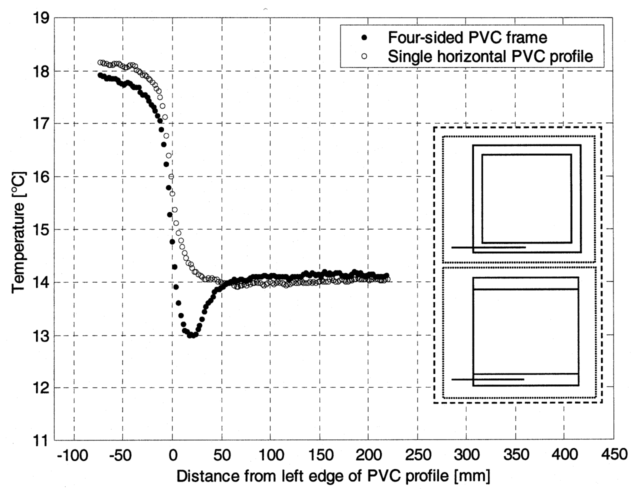

Figure 6 *Temperatures along the left lower horizontal part of the four-sided one-inch PVC frame compared to the surface temperatures along a line of the lowest one-inch profile in the configuration made up of two separate horizontal profiles; experimental uncertainty is estimated to be ±0.5°C (Griffith and Arasteh 1999).*

of the one-inch square frame compared to the temperature along the middle of one single horizontal PVC profile (mounted in the configuration of two horizontal profiles shown in Figure 3). The horizontal axis shows the distance from the left edge of the PVC profiles in millimeters, and the vertical axis shows the temperature in °C.

Figures 7, 8, and 9 show the same temperature line plots for the two-inch frame and profile sections as are shown in Figures 4, 5, and 6 for the one-inch sections. In Figure 7, which shows surface temperatures down the middle of the two-inch

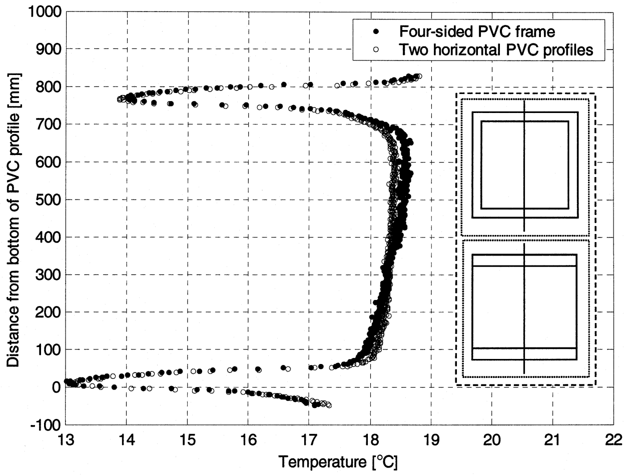

Figure 7 *Surface temperatures down the middle of the two-inch square frame compared to the temperatures along the middle of the configuration made up to two two-inch horizontal profiles. Experimental uncertainty is estimated to be ±0.5°C (Griffith and Arasteh 1999).*

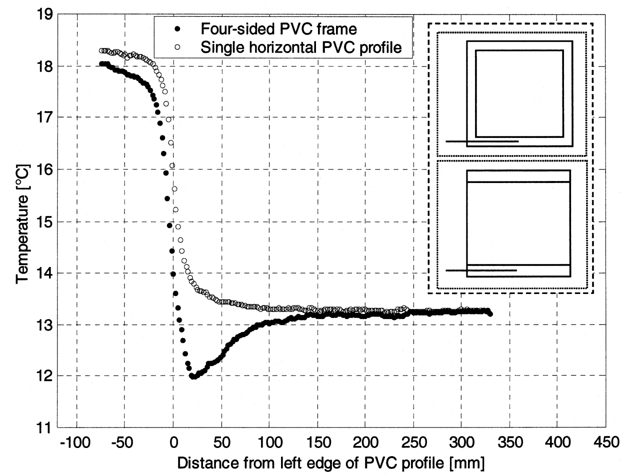

Figure 9 *Temperatures along the left lower horizontal part of the four-sided two-inch PVC frame compared to the surface temperatures along the middle of the lowest two-inch profile in the configuration made up of two separate horizontal profiles. Experimental uncertainty is estimated to be ±0.5°C (Griffith and Arasteh 1999).*

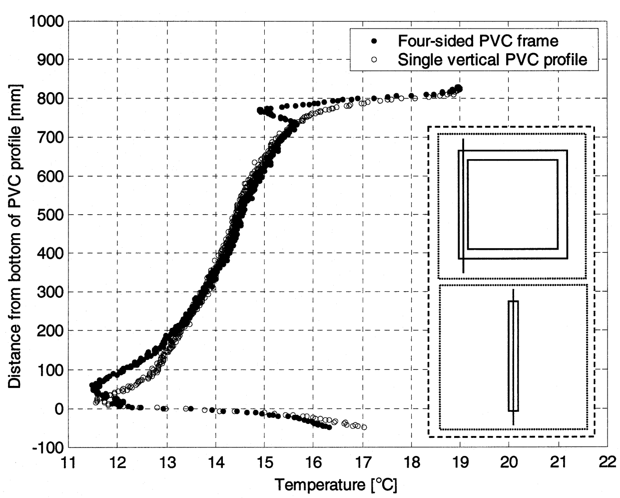

Figure 8 *Temperatures along the vertical part of the four-sided two-inch PVC frame compared to the surface temperatures of a single vertical two-inch PVC profile; experimental uncertainty is estimated to be ±0.5°C (Griffith and Arasteh 1999).*

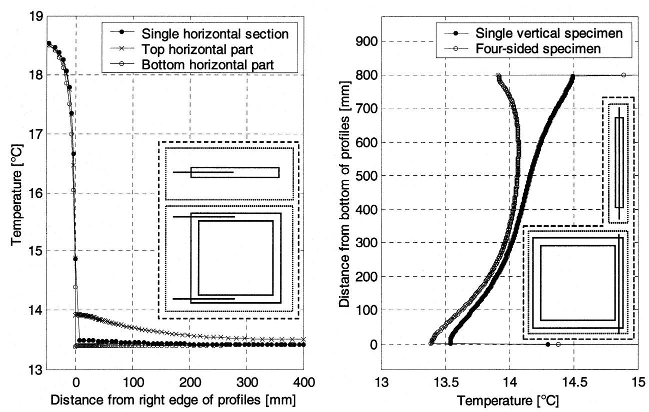

Figure 10 *This figure compares surface temperatures for the one-inch thermally broken aluminum frames. The left graph shows the temperatures along the top and bottom horizontal parts of the four-sided one-inch frame compared to the surface temperatures along the middle of the single horizontal profile. The right graph compares the temperatures along the vertical part of the four-sided frame to the surface temperatures of the single vertical one-inch profile.*

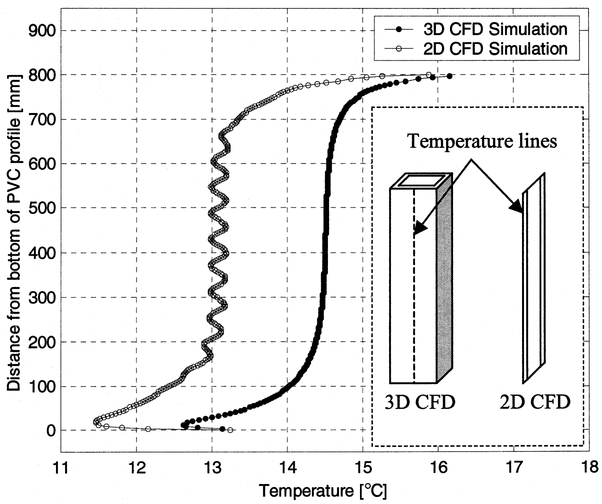

Figure 11 *Temperature distribution on the middle of the indoor side of the vertical three-dimensional PVC frame and a two-dimensional model of the PVC frame.*

square frame compared to the temperatures down the middle of the two two-inch horizontal PVC profiles, the lower PVC section extends from 0 mm to 50.8 mm, and the upper PVC section extends from 749.2 mm to 800 mm.

Figure 10 compares surface temperatures for the one-inch thermally broken aluminum specimens. The left graph shows the surface temperatures along the top and bottom horizontal parts of the four-sided one-inch frame (the corner regions) compared to the surface temperatures along the middle of a single horizontal profile. The horizontal axis shows the distance from the left edge of the thermally broken aluminum profiles in millimeters. The vertical axis shows the surface temperatures in °C. The right graph compares the temperatures along the middle of one vertical part of the four-sided frame to the surface temperatures of the middle of the single vertical one-inch section. The vertical axis shows the distance from the bottom of the profile; the bottom of the profile is at 0 mm, and the top is at 800 mm. The horizontal axis shows the surface temperatures in °C. We do not have similar plots for the two-inch thermally broken aluminum frame because that section did not converge using a stationary solution procedure, and a transient solution procedure was too time consuming.

Complex Flow

From studies on natural convection in glazing cavities we know that secondary flow may appear for certain geometries and boundary conditions (Zhao et al. 1997; Wright and Sullivan 1994). In Figure 11, we see the indoor surface temperatures of a two-dimensional model of the one-inch vertical PVC. frame compared to the surface temperatures of the middle of the three-dimensional one-inch vertical PVC frame. Both data sets are from CFD simulations. The horizontal axis shows the surface temperatures in °C and the vertical axis the accumulated distance from the bottom edge of the PVC sections in mm. Secondary flow was not observed for the vertical two-inch frame.

TABLE 4
Results for Different Simulations of PVC Window Frame Sections from the CFD Program and the Conductive Heat Transfer Program

Simulation Description (PVC Sections)	1-Inch Sections, U-Factor, W/m^2K	2-Inch Sections, U-Factor, W/m^2K
2D Section, ASHRAE (THERM)	2.29	2.53
2D Section, CEN (THERM)	2.16	2.19
3D Horizontal Section (CFD)	2.34	2.40
3D Vertical Section (CFD)	2.12	2.24
3D Four-Sided Frame (CFD)	2.24	2.33*

*This case did not converge using a stationary solution procedure. This is the value toward which the heat flow seems to converge if the problem runs for a long time using a transient solution procedure.

TABLE 5
Results for Different Simulations of Thermally Broken Aluminum Window Frame Sections from the CFD Program and the Conductive Heat Transfer Program

Simulation Description (Aluminum Sections)	1-Inch Sections, U-Factor, W/m^2K	2-Inch Sections, U-Factor, W/m^2K
2D Section, ASHRAE (THERM)	2.46	2.65
2D Section, CEN (THERM)	2.31	2.27
3D Horizontal Section (CFD)	2.52	2.56
3D Vertical Section (CFD)	2.28	2.38
3D Four-Sided Frame (CFD)	2.42	N/A

U-Factors

Table 4 summarizes the U-factor calculations for the different PVC frame sections, and Table 5 summarizes similar results for thermally broken aluminum frames. Both tables include simulation results from the CFD program and

THERM. No experimental results are included because the heat-transfer rates through the specimens were not measured. For the THERM simulations, correlations to calculate convective and radiant heat transfer in the air cavities were used. Correlations from both ASHRAE 142P (ASHRAE 1996) and ISO/DIS 10077-2 (CEN 1998) were tested. Note that the heat convection correlations in the proposed ISO 15099 (ISO 1999) are the same for air cavities in frames as the correlations used in ASHRAE 142P and that the radiation correlation for air cavities used in ASHRAE 142P is in fairly good agreement with the correlation proposed in ISO 15099 for $H/L > 1$ (Roth 1998).

For the CFD simulations, symmetry boundary conditions were used to reduce the number of computational cells and to reduce computation time. To ensure that the resolution in the discretization of the geometry was high enough, some grid sensitivity tests were performed. Some of these were not performed on the final geometries but on simpler sections that represent one part of the more complex geometries. For instance, for a two-dimensional cavity with an aspect ratio of $H/L = 40$, we found that an equispaced mesh of 25×200 was sufficient (a mesh with 45×450 nodes resulted in a change of Nusselt number by 1%). One test was also performed on a three-dimensional, horizontal, two-inch section. The number of nodes was increased both within the solid materials and in the air cavity. The refinement resulted in a change of only 0.3% in the total heat-transfer through the test specimen. The boundary conditions in this test were identical to the boundary conditions in the final simulations. We also tried to increase the number of rays traced in the radiant heat-transfer algorithm and found that doubling the number of rays in both directions only changed the total heat transfer by 0.2% (with the other parameters left constant). For the THERM simulations, we verified the influence of mesh density on U-factor for all sections by successively refining the mesh.

For both the CFD and THERM simulations, the U-factor was determined by calculating the heat flow through the warm side of the specimen and dividing that by the surface area and difference between the external and internal air temperatures. The temperatures on the internal wall surfaces in the cavity used for calculating the convection and radiation effects from the correlations in THERM were determined through several simulations and then adjusting the surface temperature.

DISCUSSION

In this discussion we analyze the differences between four-sided and single vertical and horizontal frame sections. We are interested in determining the limitations of treating a complete (four-sided) window frame with internal cavities as if it were made up of simple jamb sections, that is, dividing the complete frame into its separate parts and simulating them by themselves instead of simulating the complete frame or using simple THERM/NFRC or CEN models.

Surface Temperature

Figures 4 through 9 compare the surface temperatures of four-sided sections with those of single vertical and horizontal sections. All of these figures are based on results from the IR lab only; no CFD results are included. From Figures 4 and 7, we see that the temperatures of the middle of the four-sided frames compare well with the temperatures of the middle of the horizontal profiles. This means that the temperature differences between the upper and lower profiles of the four-sided PVC sections are not a result of cold air flowing to the bottom profile but rather of natural convection effects on the warm side, changing from top to bottom. For the CFD simulations, which used a constant surface heat-transfer coefficient, we found that the warm-side surface temperature for the four-sided PVC frame sections was the same at the middle of the top and bottom profiles (edge/corner effects are discussed below).

For the vertical sections, shown in Figures 5 and 8, there is somewhat more discrepancy between the surface temperatures of a single section and of a four-sided section. For the two-inch profiles, this difference is mostly limited to the area near the top and bottom of the frames (the corner regions); for the middle parts of the sections, the shapes of the temperature curves are almost identical. For the one-inch sections, there is a smaller difference overall, but the shapes of the curves seem to be a little different. This difference might be a result of local variation in the cold side convection effects caused by the difference in overhanging XEPS, see Figure 1.

For the thermally broken aluminum sections we have only CFD results. Figure 10 compares the surface temperatures of different one-inch specimens. We find that there are smaller temperature gradients on the surfaces for these specimens than for the PVC sections. This is a result of the high conductivity of aluminum. This high conductivity is probably also the reason for the temperatures being higher on the top horizontal part of the four-sided section than on the bottom. This temperature difference is not only limited to the edges but persists throughout the profiles. The high conductivity also prevents local surface temperature effects (local maximum and minimum values) such as those we find on the PVC sections.

Corner Effects for PVC Sections

From Figure 6, we see that the corner region of the one-inch four-sided PVC frame specimen extends about 60 mm into the horizontal part of the bottom frame, which also is what we find from the CFD simulations. Figure 9 shows that for the two-inch four-sided PVC frame, the corner region extends to about 250 mm, which is the same as what we find from the CFD simulation. For the top horizontal profile in the four-sided frames (not shown in any of the figures), these distances are about the same.

U-Factors

Because heat-transfer simulations are usually performed to generate U-factors for use in rating window frames, it is useful to compare our CFD simulations with the usual way of calculating window frame U-factors, by using conduction analysis software. Table 4 shows calculated U-factors for all PVC frames, and Table 5 shows U-factors for thermally broken aluminum frames. By studying the CFD results only, we find that there is a difference of about 0.2 W/m^2K between the horizontal and vertical profile U-factors. A difference between horizontal and vertical profiles is also anticipated from natural convection correlation studies that show that the Nusselt number is higher for square cavities than for cavities with a high aspect ratio (Raithby and Hollands 1998). The CFD simulations also seem to indicate that the U-factor of a complete (or four-sided) window frame can be found by calculating the average of the horizontal and vertical profile U-factors. This agrees with the recent findings of Haustermans (2000), who measured in a guarded hot box the U-factors of real thermally broken aluminum window frames with internal cavities. These experiments measured both four-sided window frames and single vertical and horizontal sections. Haustermans (2000) also tried to close the internal cavities of four-sided thermally broken aluminum frames; he found that closing the internal cavities at the corners had no significant influence on the U-factor.

Looking at the results from THERM, which used correlations to simulate the natural convection and radiation effects inside the cavities, we find that results differed depending on which correlations we used. Comparing the results from ASHRAE and CEN, we find that the ASHRAE correlations give higher U-factors than the CEN correlations. Further, we find that ASHRAE U-factors compare well with the results of the three-dimensional horizontal sections simulated with the CFD program, and the CEN U-factors compare well with the results of the vertical three-dimensional profiles simulated with CFD. The THERM simulations are two-dimensional. Thus, the simulated cases look like the specimens shown in Figure 1. Therefore, we would expect the U-factors from the THERM simulations to lie closest to the horizontal CFD result, as the ASHRAE correlation results do. However, as reported by Gustavsen (1999), the CEN correlation for natural convection more closely resembles natural convection in high-aspect-ratio cavities than in square cavities. Therefore, the result we found, in which the CEN U-factor is closer to the U-factor from the vertical frame CFD simulations, is also to be expected.

Treatment of Window Frames in Components

Modeling an entire window frame with internal cavities is a complex task and may require substantial computer resources and simulation time. Therefore, it is helpful to investigate whether frame cavities can be modeled at separate vertical and horizontal cavities even when they may be joined to make a continuous cavity in a four-sided frame.

Above, we studied warm-side surface temperatures of various frame sections using IR thermography and found that, except at the corner regions, the top and bottom parts of the four-sided PVC frames have similar surface temperature patterns. That is, the surface temperatures of the top and bottom profiles would be the same if the warm side surface natural convection effects were constant along the frame section. In addition, the surface temperatures of the vertical parts of the four-sided PVC sections compared well to the surface temperature of the single vertical PVC sections, excluding corner regions. However, the discrepancies in temperature patterns for the thermally broken aluminum specimens are larger and not limited only to small corner regions. Therefore, complete four-sided window frames will have to be simulated to find local temperature effects. However, if we look at the U-factor results, it seems reasonable to assume that the U-factor of a complete window frame can be found by calculating the average of the respective horizontal and vertical parts. This appears to be valid for both PVC frames and thermally broken aluminum frames.

Heat Transfer

Most correlations used today for finding the thermal performance (U-factor) of window frames are based on two-dimensional studies (both radiation and natural convection correlations). However, for vertical three-dimensional window frames, two dimensions cannot be presumed without errors in the final U-factor. These errors are a result of the small width-to-length aspect ratio of the internal frame cavities. Figure 11, for instance, shows that the secondary flow that exists in a two-dimensional, $W/L \rightarrow \infty$, cavity does not exist in a three-dimensional cavity where $W/L = 1$. The possible lack of secondary flow and the constraint imposed on the air flow in the cavity by the added vertical walls in a real three-dimensional cavity will probably decrease natural convection effects.

CONCLUSIONS

Based on our experiments and numerical simulations of heat flow through simple window frame sections we draw the following conclusions:

- Infrared thermography can be used to accurately measure the surface temperatures of window frames with internal cavities; these data can be used to compare natural convection effects in four-sided window frames with convection effects found in single vertical and horizontal window frames.
- CFD tools are useful for evaluating natural convection in the internal cavities of window frames.
- Although more investigations are needed, especially for more realistic frame sections (and those with glazing), it is reasonable to proceed using the assumption that convection in a complete window frame with joined, open internal cavities can be modeled by separating horizontal and vertical cavities; this approach yields reasonably

accurate predictions for the mean U-factor of entire frame sections. Accurate modeling of corner regions will still, however, require joining horizontal and vertical cavities.

- Traditional heat-conduction simulation tools, such as THERM, can still be used with good accuracy when calculating window frame U-factors. This statement is valid if the correct convective heat-transfer correlations are used for the internal cavities of the window frames, keeping the orientation of the frames in mind.

FUTURE RESEARCH

This work was conducted to extend our insight into heat transfer in window frame sections with internal cavities. Here, we only consider simple frame sections with one internal cavity. In practice, however, different effects are highly coupled, so to get more information about window frames with internal cavities, we need to consider variable heat-transfer coefficients for the surfaces (or model air flow at the surface) and to consider more realistic frames with more than one internal cavity, window frames with glazing, and frame sections with irregular (not rectangular) cavities. Finally, further investigation is needed to determine accurate correlations for natural convection in air enclosures with a high vertical aspect ratio ($H/L > 5$) and a low horizontal aspect ratio ($W/L \sim 1$).

ACKNOWLEDGMENTS

This work was supported by Hydro Aluminum and the Assistant Secretary for Energy Efficiency and Renewable Energy, Office of Building Technology, State and Community Programs, Office of Building Systems of the U.S. Department of Energy under Contract No. DE-AC03-76SF00098.

REFERENCES

ASHRAE. 1996. Draft BSR/ASHRAE Standard 142P, Standard method for determining and expressing the heat transfer and total optical properties of fenestration products. Atlanta: American Society of Heating, Refrigerating and Air-conditioning Engineers, Inc.

CEN. 1998. Draft prEN ISO 10077-2—Thermal performance of windows, doors and shutters—Calculation of thermal transmittance—Part 2: Numerical method for frames. Brussels: European Committee for Standardization.

ElSherbiny, S.M., G.D. Raithby, and K.G.T. Hollands. 1982. Heat transfer by natural convection across vertical and inclined air layers. *Journal of Heat Transfer*, Transactions of the ASME, 104:96-102.

Finlayson, E., R. Mitchell, D. Arasteh, C. Huizenga, and D. Curcija. 1998. *THERM 2.0: Program description. A PC program for analyzing the two-dimensional heat transfer through building products*. Berkeley: University of California.

Fluent. 1998. *FLUENT 5 User's Guide*. Lebanon, UK: Fluent Incorporated.

Griffith, B.T., and D. Arasteh. 1999. Buildings research using infrared imaging radiometers with laboratory thermal chambers. In: *Proceedings of the thermosense XXI conference* (D.H. LeMieux, J.R. Snell, eds.), Vol. 3700: 502-513. The International Society for Optical Engineering.

Griffith, B.T., F. Beck, D. Arasteh, and D. Türler. 1995. Issues associated with the use of infrared thermography for experimental testing of insulated systems. In *Thermal performance of the exterior envelopes of buildings VI*. Atlanta: American Society of Heating, Refrigerating and Air-Conditioning Engineers, Inc.

Griffith, B., E. Finlayson, M. Yazdanian, and D. Arasteh. 1998. The significance of bolts in the thermal performance of curtain-wall frames for glazed facades. *ASHRAE Transactions* 104(1B): 1063-1069.

Gustavsen, A., B.T. Griffith, and D. Arasteh. 2001. Three-dimensional conjugate computational fluid dynamics simulations of internal window frame cavities validated using infrared thermography.*ASHRAE Transactions* 107(2).

Gustavsen, A. 1999. Comparison of Nusselt number correlations for convection heat transfer in a cavity. In *Proceedings of the 5th symposium on building physics in the Nordic countries*, Vol. 1:201-208. Göteborg, Sweden: Chalmers University of Technology.

Haustermans, L. 2000. Heat transfer in aluminium window frame profiles. Computer modelling and hot box measurements. Master of science thesis., Departement Burgerlijke Bouwkunde, Katholieke Universiteit Leuven, Leuven, Belgium.

ISO. 1999. Draft Standard ISO 15099—*Thermal performance of windows, doors and shading devices—Detailed calculations*. Geneva, Switzerland: International Organisation for Standardisation.

ISO. 1998. Draft Standard ISO/DIS 12567—*Thermal performance of doors and windows—Determination of thermal transmittance by hot box method*. Geneva, Switzerland: International Organisation for Standardisation.

Lee, Y., and S.A. Korpela. 1983. Multicellular natural convection in a vertical slot. *Journal of Fluid Mechanics* 126:91-121.

Patankar, S.V. 1980. *Numerical heat transfer and fluid flow.* Washington, D.C.: Hemisphere.

Raithby, G.D., and K.G.T. Hollands. 1998. Natural convection. In *Handbook of heat transfer*, 3d ed. (W.M. Rosenhow, J.P. Hartnett, Y.I. Cho, eds.), pp. 4.1-4.99. McGraw-Hill.

Roth, H. 1998. Comparison of thermal transmittance calculation methods based on ASHRAE and CEN/ISO standards. Master of science thesis, Department of

Mechanical and Industrial Engineering, University of Massachusetts, Amherst.
Shewen, E., K.G.T. Hollands, and G.D. Raithby. 1996. Heat transfer by natural convection across a vertical air cavity of large aspect ratio. *Journal of Heat Transfer, Transactions of the ASME*, Vol. 118:993-995.
Türler, D., B.T. Griffith, and D. Arasteh. 1997. Laboratory procedures for using infrared thermography to validate heat transfer models. In *Insulation materials: Testing and applications*, 3d vol., ASTM STP 1320 (R.S. Graves, R.R. Zarr, eds.). American Society for Testing and Materials.
Versteeg, H.K., and W. Malalasekera. 1995. *An introduction to computational fluid dynamics. The finite volume method*. Essex, England: Addison Wesley Longman Limited.
Wright, J.L. and H.F. Sullivan. 1994. A two-dimensional numerical model for natural convection in a vertical, rectangular window cavity. *ASHRAE Transactions* 100(2): 1193-1206.
Yin, S.H., T.Y. Wung, and K. Chen. 1978. Natural convection in an air layer enclosed within rectangular cavities. *International Journal of Heat and Mass Transfer* 21: 307-315.
Zhao, Y., D. Curcija, and W.P. Goss. 1997. Prediction of the multicellular flow regime of natural convection in fenestration glazing cavities. *ASHRAE Transactions* 103(1):1009-1020.
Zhao, Y. 1998. Investigation of heat transfer performance in fenestration system based on finite element methods. Ph.D. dissertation, Department of Mechanical and Industrial Engineering, University of Massachusetts.